PERGAMON

Journal of the Mechanics and Physics of Solids
51 (2003) 1287 – 1304

JOURNAL OF THE
MECHANICS AND
PHYSICS OF SOLIDS

www.elsevier.com/locate/jmps

Brittle fracture dynamics with arbitrary paths I. Kinking of a dynamic crack in general antiplane loading

M. Adda-Bedia[a,*], R. Arias[b]

[a]*Laboratoire de Physique Statistique de l'Ecole Normale Supérieure, 24 rue Lhomond, F-75231 Paris Cedex 05, France*
[b]*Departamento de Física, Facultad de Ciencias Físicas y Matemáticas, Universidad de Chile, Casilla 487-3 Santiago, Chile*

Received 11 April 2002; accepted 29 January 2003

Abstract

We present a new method for determining the elasto-dynamic stress fields associated with the propagation of anti-plane kinked or branched cracks. Our approach allows the exact calculation of the corresponding dynamic stress intensity factors. The latter are very important quantities in dynamic brittle fracture mechanics, since they determine the crack path and eventual branching instabilities. As a first illustration, we consider a semi-infinite anti-plane straight crack, initially propagating at a given time-dependent velocity, that changes instantaneously both its direction and its speed of propagation. We will give the explicit dependence of the stress intensity factor just after kinking as a function of the stress intensity factor just before kinking, the kinking angle and the instantaneous velocity of the crack tip.

Keywords: A. Crack branching and bifurcation; Dynamic fracture; Stress intensity factors; B. Crack mechanics; C. Analytic functions

1. Introduction

In many experimental situations, cracks propagate by following curved or kinked paths (Broberg, 1999; Freund, 1990; Lawn, 1993). Another well-known phenomenon in brittle crack propagation is the possible emergence from a single crack tip of two

* Corresponding author. Present address: DAMTP, Center for Mathematical Sciences, Wilberforce Road, Cambridge CB3 0WA, UK. Fax: +44-1223-765900.

E-mail address: m.adda-bedia@damtp.cam.ac.uk (M. Adda-Bedia).

doi:10.1016/S0022-5096(03)00022-X

or more branches. Experiments in PMMA and glass plates (Ravi-Chandar and Knauss, 1984; Sharon and Fineberg, 1996, 1999) have shown that this phenomenon occurs for fast single propagating cracks after they surpass a critical velocity that is a fraction of the Rayleigh wave speed of these materials. Above this critical speed, a dynamical instability sets in marked by the appearance of micro-branches, roughness of the crack surfaces, sound emission, and eventual macro-branches at higher speeds.

The knowledge of the instantaneous stress fields in the vicinity of the crack tip is necessary for the theoretical prediction of a crack path. Therefore, the determination of the elasto-dynamic fields associated with the propagation of kinked or branched cracks is an unavoidable step in the study of brittle fracture dynamics. Unfortunately, a general solution to the dynamical kinking or branching problem is not available yet. Up to now, efforts have been dedicated to the study of elasto-static solutions of kinked or branched cracks (Sih, 1965; Amestoy and Leblond 1992; Leblond, 1989). Also, in addition to the well established solutions of straight crack propagation (Freund, 1990; Kostrov, 1966; Kostrov, 1975; Eshelby, 1969), the only known elasto-dynamic solutions related with the kinking or branching problem deal with a semi-infinite crack that starts to propagate from rest by kinking or branching under the action of a stress pulse loading (Dempsey et al., 1982; Burgers, 1982, 1983).

The aim of this paper is to present a new method to calculate the dynamic stress intensity factors associated with the propagation of anti-plane kinked or branched cracks. As a first application, we consider the dynamic kinking of an initially semi-infinite straightly propagating crack. We will give the explicit dependence of the stress intensity factor just after kinking as a function of the stress intensity factor prior to kinking, the kinking angle and the instantaneous velocity of the crack tip. This method can be generalized to the case of an initially propagating anti-plane crack that branches into two or more cracks. The case of two cracks that branch symmetrically from a single crack will be the subject of the next application of our method.

The paper is organized as follows. In the next section, we introduce our approach to the dynamical kinked crack problem under mode III loading, and we derive the corresponding model problem. In Section 3, we detail the self-similar solution that it admits. The present work can be considered as an extension of the self-similar analysis of dynamic crack growth initiated by Broberg (Broberg, 1999) and Achenbach (Dempsey et al., 1982) among others. A detailed discussion of the analysis of self-similar mixed boundary value problems in elasto-dynamics can also be found in the work of Willis (1973). In the present case, the self-similar solution of the dynamic crack kinking problem is given by an integral representation, which is a convolution between a known kernel and a harmonic function, which is determined by the real part of a holomorphic function. In Section 4, the harmonic function is mapped into an upper complex half-plane, with boundary conditions on the real axis, and an intermediate exact solution is given. In Section 5, the numerical resolution of the integral equation is presented. The results for the stress intensity factor just after kinking are given for arbitrary angles and velocities. Finally, we discuss our results, especially the difference between our solution and the elasto-static solution, and the consequences of this discrepancy for the selection of crack paths in quasi-static situations.

2. The dynamical kinked crack under mode III loading

Consider an elastic body which contains a half-plane kinked crack but which is otherwise unbounded (see Fig. 1). Introduce a cylindrical coordinate system (r,θ,z) so that the z-axis lies along the crack edge. The upward (resp. downward) semi-infinite crack surface occupies the half-plane $\theta=\pi$ (resp. $\theta=-\pi$). Suppose that the material is subjected to a loading which produces a state of anti-plane shear deformation in the body. Thus the only nonzero component of displacement is the z-component $u_z(r,\theta,t)\equiv w(r,\theta,t)$, which is independent of z.

The scenario of crack kinking is developed as follows. A semi-infinite straight crack that propagates at a speed $v(t)$ for $t<-\tau$ (with $\tau\to 0^+$) suddenly stops at $t=-\tau$. At $t\to 0^+$, the crack kinks locally with a kinking angle equal to $\lambda\pi$, with $-1<\lambda<1$. For $t>0^+$, the new branch propagates straightly at a velocity $v'(t)$, following this new direction. The magnitudes of the crack speeds v and v' are restricted by $0<v<c$ and $0<v'<c$, where c denotes the elastic shear wave speed. It is well known (Freund, 1990; Kostrov, 1966, 1975; Eshelby, 1969) that the mode III dynamic stress intensity factor, $K(t)$, of the straight crack prior to kinking is related to the rest stress intensity factor, $K_0(t)$, of the same configuration by

$$K(t)=k(v)K_0(t), \tag{1}$$

where $k(v)$ is a universal function of the instantaneous crack tip speed given by

$$k(v)=\sqrt{1-v/c}. \tag{2}$$

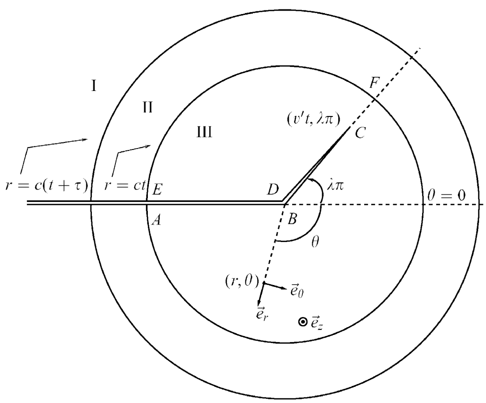

Fig. 1. Schematic representation of an anti-plane kinked crack problem. A half-plane crack that propagates at a speed v for $t<-\tau$ suddenly stops at $t=-\tau$, at $r=0$. For $t>0$, the new branch propagates straightly at a velocity v', following the direction $\lambda\pi$. The orthonormal basis $(\vec{e}_r,\vec{e}_\theta,\vec{e}_z)$ corresponding to the cylindrical coordinate system (r,θ,z) is shown. The cylindrical waves originated at the crack's arrest $(r=c(t+\tau))$ and at the start of kink propagation $(r=ct)$ divide the material into three regions. In the region labelled I, the stress field comes only from the dynamical straight crack propagation, since the effects of the crack's arrest and the crack's kinking are not experienced there. The region II is influenced by the crack arrest only, thus the stress field there is a static one (Freund, 1990; Eshelby, 1969). It is only the region III that is influenced by the crack's kinking. Thus, one has to solve the kinked crack problem only in this latter region.

We are interested in the dynamic stress intensity factor just after kinking, K', as a function of the kinking angle, the crack tip speeds (prior and after kinking), the material parameters and of the applied load. According to our description of crack kinking, K' should be defined as

$$K'(\lambda, v, v', c, \ldots) = \lim_{\tau\to 0^+} \lim_{t\to 0^+} \lim_{(r-v't)\to 0^+} \sqrt{2\pi(r - v't)}\sigma_{\theta z}(r, \lambda\pi, t). \tag{3}$$

We emphasize the importance of the order in which the limits in Eq. (3) should be taken. The decomposition of the crack kinking process as described above imposes that the limit $t \to 0^+$ must be taken before the limit $\tau \to 0^+$.

In the limit $t \to 0^+$, the length of the kinked part of the crack is vanishingly small, so that the breaking process after kinking occurs in the region determined by the square root singular stress intensity factor field of the semi-infinite crack. Therefore, the applied loads on the kink involve only the stress intensity scale, and the physical system does not involve either a characteristic time scale or a characteristic length scale. This imposes that the stress intensity factor just after kinking should be written as

$$K' = H_{33}(\lambda, v/c, v'/c)K_0, \tag{4}$$

where H_{33} is an unknown dimensionless function of the kinking angle $\lambda\pi$ and of the crack tip speeds v and v'. As in the quasi-static case (Leblond, 1989), the function H_{33} is universal in the sense that it does not depend either on the loading configuration or on the geometry of the body. Effectively, in the limits $t \to 0^+$ and $\tau \to 0^+$ that we consider, the dynamic kinking problem does not involve incoming radiation effects, so it is always equivalent to a crack propagating in an unbounded body. On the other hand, due to the absence in linear elasticity theory of intrinsic times or length scales, this problem becomes of general validity since it is not necessary for the crack or the kink to be straight. Effectively, we can generalize the quasi-static analysis (Leblond, 1989) so that Eq. (4) is also valid for dynamic curved cracks; H_{33} does not depend on the local curvature of the crack prior or after kinking.

For the mode III case, when the initial crack stops, a static stress distribution is restored behind a wave front that propagates from the crack tip at the shear wave speed (Eshelby, 1969), (see Fig. 1). Thus for $t > 0$, the propagation of the kinked crack occurs within a stationary stress field. Our kinking problem is then equivalent to solving the problem of a kink that emerges from a pre-existing stationary straight crack, and that started to propagate at time $t = 0^+$, in the direction $\lambda\pi$, with a velocity v', under the action of a time-independent loading. Moreover, in order to compute the stress intensity factor just after kinking given by Eq. (4), it is enough to solve this problem by considering the static stress distribution $\sigma^s_{\theta z}(r, \theta)$, which in the vicinity of the stationary initial crack tip has a square root singular stress intensity factor field given by (Williams, 1952)

$$\sigma^s_{\theta z}(r, \theta) = \frac{K_0}{\sqrt{2\pi r}} \cos\frac{\theta}{2}, \tag{5}$$

where K_0 is the rest stress intensity factor of the crack tip prior to kinking, which is related to the dynamic stress intensity factor, K, just before kinking through Eq. (1).

A straightforward consequence of these previous arguments is that the universal function H_{33} must be independent of the velocity prior to kinking

$$H_{33}(\lambda, v/c, v'/c) \equiv H_{33}(\lambda, v'/c). \tag{6}$$

Also, it is clear that H_{33} should satisfy the following property

$$\lim_{\lambda \to 0} H_{33}(\lambda, v'/c) = k(v'), \tag{7}$$

for all values of v' (Kostrov, 1966; Eshelby, 1969).

2.1. The model problem of dynamic crack kinking

The process of crack advance in the situation depicted in Fig. 1 can be viewed as the process of negating the traction distribution on the newly broken surface produced by the stress field distribution of the stationary crack given by Eq. (5). For $t < 0$, it is assumed that the crack is at rest and that the material is loaded according to Eq. (5). As the crack advances for $t > 0$, the component of displacement $w(r, \theta, t)$ satisfies the wave equation in two-space dimensions and time,

$$\Delta w \equiv \frac{1}{r}\frac{\partial}{\partial r}\left(r\frac{\partial w}{\partial r}\right) + \frac{1}{r^2}\frac{\partial^2 w}{\partial \theta^2} = \frac{1}{c^2}\frac{\partial^2 w}{\partial t^2}, \tag{8}$$

with the boundary conditions on the displacement field $w(r, \theta, t)$, for $r \leqslant ct$, given by

$$\sigma_{\theta z}(r, \pm\pi, t) = 0, \tag{9}$$

$$\sigma_{\theta z}(r < v't, \lambda\pi \pm \varepsilon, t) = 0, \tag{10}$$

$$w(ct, \theta, t) = \frac{2K_o}{\mu}\sqrt{\frac{ct}{2\pi}} \sin\frac{\theta}{2}. \tag{11}$$

Here (and elsewhere), ε is a vanishingly small positive constant, μ is the shear modulus, and

$$\sigma_{\theta z} = \frac{\mu}{r}\frac{\partial w}{\partial \theta}. \tag{12}$$

Condition (11) is a consequence of the continuity of the displacement field $w(r, \theta, t)$ at the wave front $r = ct$, that follows from Eq. (5). Notice that continuity of $\sigma_{\theta z}$ across the wave front follows from continuity of the displacement $w(r, \theta, t)$ there, and from Eq. (12). Moreover, there is a jump condition across the wave front $r = ct$ given by (Dempsey et al., 1982)

$$[\sigma_{rz}]_{r=ct} + \frac{\mu}{c}\left[\frac{\partial w}{\partial t}\right]_{r=ct} = 0, \tag{13}$$

where $[f]_r \equiv f(r + \varepsilon) - f(r - \varepsilon)$, with $\varepsilon \to 0$, and

$$\sigma_{rz} = \mu\frac{\partial w}{\partial r}. \tag{14}$$

Of interest is to establish the kind of singularity of the stress $\sigma_{\theta z}$ to be expected in the vicinity of the edge points B and D in Fig. 1, once the kink develops. Indeed, the Williams expansion (Williams, 1952) imposes that the singularity of this stress component in the vicinity of these edge points should be given by

$$\sigma_{\theta z}(r,\theta,t) \sim r^p \quad \text{as } r \to 0, \tag{15}$$

where

$$p = \begin{cases} \dfrac{\lambda}{1-\lambda}, & \text{for } \lambda\pi < \theta < \pi, \\ \dfrac{-\lambda}{1+\lambda}, & \text{for } -\pi < \theta < \lambda\pi. \end{cases} \tag{16}$$

Finally, the asymptotic behavior of the stress field near the propagating crack tip is given by (Freund, 1990)

$$\sigma_{\theta z}(r,\lambda\pi \pm \varepsilon,t) = \left[\frac{K'}{\sqrt{2\pi(r-v't)}} + O(\sqrt{r-v't})\right] H(r-v't) \quad \text{as } r \to v't, \tag{17}$$

with K' the stress intensity factor after kinking and H the heaviside function.

3. Resolution of the dynamic crack kinking problem

3.1. Self-similar analysis

As a solution of the elasto-dynamic problem established in Eqs. (8)–(11), scaling analysis and the linearity of the wave equation imposes the following self-similar form for the displacement field:

$$w(r,\theta,t) = \frac{K_o}{\mu}\sqrt{\frac{r}{2\pi}}\left[2\sin\frac{\theta}{2} + W(r,\theta,t)\right], \tag{18}$$

where W is a dimensionless function of its arguments. Equivalently, the stress field takes the following form:

$$\sigma_{\theta z}(r,\theta,t) = \frac{K_o}{\sqrt{2\pi r}}\left[\cos\frac{\theta}{2} + S(r,\theta,t)\right], \tag{19}$$

with

$$S(r,\theta,t) = \frac{\partial W}{\partial\theta}(r,\theta,t). \tag{20}$$

Except for the stress intensity factor scale introduced by the boundary condition (11), there is neither a characteristic length nor a characteristic time against which the independent variables r, θ and t can be scaled. Therefore, W and S can only depend on dimensionless combinations of r, θ and t. These dimensional arguments determine the displacement function W and the stress function S to be written as

$$W(r,\theta,t) = W(\chi,\theta), \qquad S(r,\theta,t) = S(\chi,\theta), \tag{21}$$

where

$$\chi \equiv \frac{ct}{r}, \qquad \chi \geqslant 1. \tag{22}$$

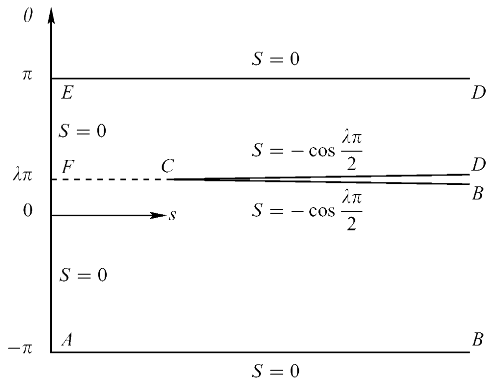

Fig. 2. The (s, θ)-plane, with $s \geqslant 0$ and $-\pi \leqslant \theta \leqslant \pi$, that maps the region III of (r, θ, t)-space, corresponding to $r \leqslant ct$, $-\pi \leqslant \theta \leqslant \pi$, and $t > 0$ (see Fig. 1).

Using Eqs. (8) and (18), and taking into account the explicit dependence of χ on r and t, one finds that W satisfies the following partial differential equation:

$$(\chi^2 - 1)\frac{\partial^2 W}{\partial \chi^2} + \frac{\partial^2 W}{\partial \theta^2} + \frac{1}{4}W = 0. \tag{23}$$

Let us make a new change of variable $\chi(s)$, by using the well-known Chaplygin's transformation (Dempsey et al., 1982; Broberg, 1999; Freund, 1990)

$$\chi(s) \equiv \cosh s, \qquad s \geqslant 0. \tag{24}$$

In Fig. 2, the transformation from the coordinates system (r, θ, t) to the (s, θ)-plane is shown. Thus, in the space of coordinates (s, θ), Eq. (23) becomes

$$\frac{\partial^2 W}{\partial s^2} - \coth s\, \frac{\partial W}{\partial s} + \frac{\partial^2 W}{\partial \theta^2} + \frac{1}{4}W = 0. \tag{25}$$

The boundary conditions (9)–(11) can be easily re-expressed as boundary conditions on the displacement and stress functions W and S. In the new coordinates system, they take the form

$$W(s = 0, \theta) = 0, \tag{26}$$

$$S(s, \theta = \pm\pi) = 0, \tag{27}$$

$$S(s > b, \theta = \lambda\pi \pm \varepsilon) = -\cos\frac{\lambda\pi}{2}, \tag{28}$$

where

$$b \equiv \cosh^{-1}(c/v'). \tag{29}$$

The Williams expansion imposes that the asymptotic behavior of $\sigma_{\theta z}(r, \theta, t)$ in the vicinity of the edge points B and D should be weaker than the square root singularity;

the singularity of the stress field there is given by Eqs. (15) and (16). Therefore, in the vicinity of B and D the function $S(s,\theta)$ must satisfy

$$S(s,\theta) = -\cos\frac{\theta}{2} + O\left(\exp - \left(p+\frac{1}{2}\right)s\right) \quad \text{as } s \to +\infty, \tag{30}$$

with p given by Eq. (16). On the other hand, the asymptotic behavior near the crack tip, given by Eq. (17), imposes the following asymptotic behavior in the (s,θ)-plane:

$$S(s,\lambda\pi \pm \varepsilon) = -\cos\frac{\lambda\pi}{2} + \left[\frac{K'}{K_o}\frac{\sqrt{\coth b}}{\sqrt{b-s}} + O(\sqrt{b-s})\right] H(b-s) \quad \text{as } s \to b. \tag{31}$$

Finally, once the displacement field $w(r,\theta,t)$ is written in the form of Eqs. (18) and (21), the jump condition (13) across the cylindrical wave front $s=0$, corresponding to $r=ct$, is automatically satisfied.

3.2. Integral representation of the self-similar solution

Using the linearity of Eq. (25), it can be shown that the displacement function $W(s,\theta)$ admits solutions of the form

$$W(s,\theta) = \sinh s\, P^{-1}_{-1/2+\mathrm{i}\nu}(\cosh s)\Theta_\nu(\theta), \tag{32}$$

where ν is a complex constant, and $P^{-1}_{-1/2+\mathrm{i}\nu}$ is the associated Legendre function of the first kind (Gradshteyn and Ryzhik, 1994). On the other hand, the function Θ_ν satisfies the simple second order differential equation given by

$$\frac{\mathrm{d}^2\Theta_\nu}{\mathrm{d}\theta^2} - \nu^2\Theta_\nu = 0, \tag{33}$$

whose solution is a superposition of the functions $\sinh \nu\theta$ and $\cosh \nu\theta$. Notice that in Eq. (32), we did not take into account the solutions that contain the associated Legendre function of the second kind $Q^{-1}_{-1/2+\mathrm{i}\nu}(\cos s)$ (Gradshteyn and Ryzhik, 1994). This is due to the fact that only outgoing waves from $r=0$, corresponding to $s\to\infty$, are present in our problem. These waves are represented by the $P^{-1}_{-1/2+\mathrm{i}\nu}$ contribution. The absence of incoming radiation towards $r=0$, automatically cancels the $Q^{-1}_{-1/2+\mathrm{i}\nu}$ contribution. Using the integral representation of the associated Legendre functions given by (Gradshteyn and Ryzhik, 1994)

$$P^{\beta}_{\alpha}(\cosh s) = \sqrt{\frac{2}{\pi}}\frac{\sinh s^{\beta}}{\Gamma(\frac{1}{2}-\beta)}\int_0^s \frac{\cosh(\alpha+\frac{1}{2})s'}{(\cosh s - \cosh s')^{\beta+1/2}}\,\mathrm{d}s', \tag{34}$$

one can rewrite ($\beta=-1,\ \alpha=-1/2+\mathrm{i}\nu$), without loss of generality, the complete solution of Eq. (25) in the form

$$W(s,\theta) = \frac{2}{\pi}\int_0^s \sqrt{\cosh s - \cosh s'}\, f(s',\theta)\,\mathrm{d}s', \tag{35}$$

where $f(s,\theta)$ is an unknown function that satisfies the harmonic equation

$$\left[\frac{\partial^2}{\partial s^2}+\frac{\partial^2}{\partial \theta^2}\right] f(s,\theta)=0, \tag{36}$$

and the additional boundary condition.

$$\left[\frac{\partial}{\partial s} f(s,\theta)\right]_{s=0}=0. \tag{37}$$

It is straightforward to confirm a posteriori that the latter integral representation of $W(s,\theta)$, combined with conditions (36) and (37), is an exact solution of Eq. (25).

Also, notice that once the displacement function $W(s,\theta)$ is written in the form (35), the boundary condition (26) at the cylindrical wave front $s=0$ is automatically satisfied. The problem as it is posed now is tractable, at least numerically, because it allows the use of complex analysis and conformal mapping techniques.

3.3. Boundary conditions and asymptotic behavior

The solution of the dynamic kinking problem within the representation of Eqs. (35)–(37) of $W(s,\theta)$ is reduced to the determination of $f(s,\theta)$. Harmonicity of $f(s,\theta)$ means that it can be written as the real part of a complex function $F(\gamma=s+\mathrm{i}\theta)$, which is holomorphic inside the contour *DCBAED* (see Fig. 2):

$$f(s,\theta)=\mathrm{Re}[F(\gamma)]\equiv\frac{1}{2}[F(\gamma)+\overline{F(\gamma)}],\qquad \gamma=s+\mathrm{i}\theta. \tag{38}$$

Using Eqs. (20) and (38) and the Cauchy identities for holomorphic functions, the function $S(s,\theta)$ can be written in the form

$$S(s,\theta)=\frac{2}{\pi}\sqrt{\cosh s-1}\,\mathrm{Im}[F(\mathrm{i}\theta)]-\int_0^s\frac{\sinh s'\mathrm{Im}[F(s'+\mathrm{i}\theta)]}{\sqrt{\cosh s-\cosh s'}}\frac{\mathrm{d}s'}{\pi}. \tag{39}$$

Condition (30) implies that the stress function $S(s,\theta)$ does not diverge as $s\to+\infty$. This imposes that

$$\mathrm{Im}[F(\mathrm{i}\theta)]=0. \tag{40}$$

Using again the Cauchy relations for holomorphic functions, one finds that Eq. (40) is sufficient for satisfying the boundary condition (37). Therefore, Eq. (39) is reduced to

$$S(s,\theta)=-\int_0^s\frac{\sinh s'\,\mathrm{Im}[F(s'+\mathrm{i}\theta)]}{\sqrt{\cosh s-\cosh s'}}\frac{\mathrm{d}s'}{\pi}. \tag{41}$$

Using Eq. (41), Expansions (30) in the vicinity of the wedge points B and D are completely recovered if the function F satisfies

$$\mathrm{Im}[F(\gamma)]=\sqrt{2}\exp\left[-\frac{s}{2}\right]\cos\frac{\theta}{2}+O(\exp-(p+1)s)\quad\text{as } s\to\infty. \tag{42}$$

The asymptotic behavior of the stress function $S(s,\theta)$ near the crack tip embodied in Eq. (31) imposes a specific behavior of $F(\gamma)$ in the neighborhood of the corresponding point $\gamma_C \equiv b + \mathrm{i}\lambda\pi$. This can be obtained by an Abel inversion of Eq. (41), or by noting the equality (Gradshteyn and Ryzhik, 1994)

$$\int_0^s \frac{\sinh(s'/2)\sinh s'\,\mathrm{d}s'}{\sqrt{\cosh s - \cosh s'}(\cosh s' - \cosh b \pm \mathrm{i}\varepsilon)}$$

$$= \frac{\pi}{\sqrt{2}}\left[1 - \frac{\sqrt{2}\sinh(b/2)}{\sqrt{\cosh b - \cosh s \mp \mathrm{i}\varepsilon}}\right]. \tag{43}$$

Identifying the behavior of Eq. (43) when $s \to b$ with that of Eq. (31), one concludes that $F(\gamma)$ behaves as

$$F(\gamma) \simeq \frac{\mathrm{i}a}{\gamma - \gamma_C} + O((\gamma-\gamma_C)^0) \quad \text{as } \gamma \to \gamma_C \equiv b + \mathrm{i}\lambda\pi, \tag{44}$$

where a is a real constant related to the stress intensity factor just after kinking, K', by

$$a = \frac{\sqrt{\cosh b}}{\sinh b}\,\frac{K'}{K_o}. \tag{45}$$

Thus, the function F has a simple pole at $\gamma = \gamma_C$. Also, the higher order terms in expansion (44) of $F(\gamma)$ are prescribed by the higher order terms in expansion (31) of the stress field S in the vicinity of the crack tip. In particular, logarithmic singularities of the form $\log(b-s)$ and terms of the form $(b-s)^\mu$, with $-1/2 < \mu < 1/2$, are forbidden.

We now turn to the condition imposed on $F(\gamma)$ by the boundary conditions (27) and (28) satisfied by S. The boundary conditions (27) on S implies that $F(\gamma)$ must satisfy

$$\mathrm{Im}[F(s \pm \mathrm{i}\pi)] = 0. \tag{46}$$

The boundary condition Eq. (28) of S means that $\mathrm{Im}[F]$ satisfies the following integral equation for $s > b$:

$$\int_b^s \frac{\sinh s'\,\mathrm{Im}[F(s' + \mathrm{i}(\lambda\pi \pm \varepsilon))]}{\sqrt{\cosh s - \cosh s'}}\,\frac{\mathrm{d}s'}{\pi} = g(s) \tag{47}$$

with

$$g(s) \equiv \cos\frac{\lambda\pi}{2} - \int_0^b \frac{\sinh s'\,\mathrm{Im}[F(s' + \mathrm{i}\lambda\pi)]}{\sqrt{\cosh s - \cosh s'}}\,\frac{\mathrm{d}s'}{\pi}. \tag{48}$$

We write this integral equation differently by noticing that Eq. (47) is in the form of an Abel integral equation (Freund, 1990). Thus, one can invert Eq. (47) to obtain

$$\mathrm{Im}[F(s + \mathrm{i}(\lambda\pi \pm \varepsilon))] = \frac{1}{\sinh s}\,\frac{\mathrm{d}}{\mathrm{d}s}\int_b^s \frac{\sinh s'\,g(s')}{\sqrt{\cosh s - \cosh s'}}\,\mathrm{d}s'. \tag{49}$$

Then using Eq. (48) for $g(s')$, one finally gets

$$\sqrt{\cosh s - \cosh b}\,\mathrm{Im}\,[F(s + \mathrm{i}(\lambda\pi \pm \varepsilon))] = \cos\frac{\lambda\pi}{2} - \int_0^b \frac{\sqrt{\cosh b - \cosh s'}}{\cosh s - \cosh s'} \sinh s'\,\mathrm{Im}\,[F(s' + \mathrm{i}\lambda\pi)]\,\frac{\mathrm{d}s'}{\pi}. \tag{50}$$

The next step in solving our problem is to transform the strip geometry of Fig. 2 into a half-plane geometry by use of a conformal transformation of coordinates that is detailed in the following. The boundary conditions will be applied on the real axis of the new coordinate system.

4. Solution of the dynamic crack kinking problem

4.1. Conformal mapping

Let us map the interior of the contour $DCBAED$ in the γ-plane into the upper half-plane of a new coordinates system (ξ, η). The conformal mapping associated with this transformation is given by (Dempsey et al., 1982)

$$\gamma(\zeta) = (1+\lambda)\ln\left[\frac{1 + \xi_B\zeta + \sqrt{(1-\xi_B^2)(1-\zeta^2)}}{\zeta + \xi_B}\right] + (1-\lambda)\ln\left[\frac{1 - \xi_D\zeta + \sqrt{(1-\xi_D^2)(1-\zeta^2)}}{\zeta - \xi_D}\right] + \mathrm{i}\pi, \tag{51}$$

where $\zeta = \xi + \mathrm{i}\eta$. Fig. 3 shows the ζ-plane and the locations, on the ξ-axis, of the points corresponding to the vertices of the polygon $DCBAFED$, in the γ-plane. The conditions satisfied by ξ_B, and ξ_D are given by (Dempsey et al., 1982)

$$(1+\lambda)\,\frac{\sqrt{1-\xi_B^2}}{\xi_B} - (1-\lambda)\,\frac{\sqrt{1-\xi_D^2}}{\xi_D} = 0, \tag{52}$$

$$(1+\lambda)\cosh^{-1}\left[\frac{1}{\xi_B}\right] + (1-\lambda)\cosh^{-1}\left[\frac{1}{\xi_D}\right] = b. \tag{53}$$

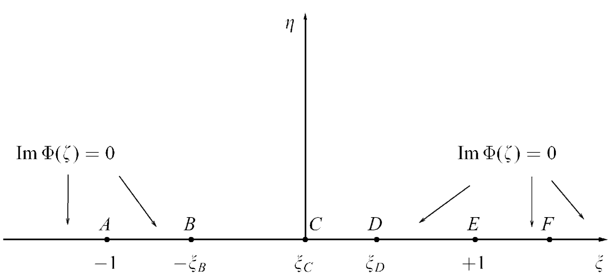

Fig. 3. The ζ-plane corresponding to the conformal mapping $\gamma(\zeta)$.

On the other hand, when $\gamma \to \gamma_C$, or equivalently $\zeta \to 0$, one has

$$\gamma(\zeta) \simeq \gamma_C + \frac{\gamma_2}{2}\zeta^2 + \frac{\gamma_3}{6}\zeta^3 + O(\zeta^4), \tag{54}$$

with

$$\gamma_2 \equiv \gamma''(0) = (1+\lambda)\frac{\sqrt{1-\xi_B^2}}{\xi_B}\left[\frac{1}{\xi_B} + \frac{1}{\xi_D}\right], \tag{55}$$

$$\gamma_3 \equiv \gamma'''(0) = 2(1+\lambda)\frac{\sqrt{1-\xi_B^2}}{\xi_B}\left[\frac{1}{\xi_D^2} - \frac{1}{\xi_B^2}\right]. \tag{56}$$

4.2. Solution in the ζ-space

We look for the analytic function $F(\gamma)$ on the new half-space, and we call it $\Phi(\zeta) \equiv F(\gamma(\zeta))$, with $\zeta = \xi + i\eta$. The function $\Phi(\zeta)$ is now holomorphic for $\mathrm{Im}[\zeta] > 0$, and the conditions it satisfies on the real axis of the ζ-plane are readily given from those of $F(\gamma)$ in the γ-plane. Eqs. (40) and (46) imply that

$$\mathrm{Im}[\Phi(\xi)] = 0 \quad \text{for } \xi > \xi_D \text{ or } \xi < -\xi_B. \tag{57}$$

Moreover, the function $\Phi(\zeta)$ should also satisfy

$$\lim_{|\zeta|\to\infty} \mathrm{Im}[\Phi(\zeta)] = 0. \tag{58}$$

This condition follows from the fact that $|\zeta| \to \infty$ corresponds to a point lying on the imaginary axis of the γ-plane ($s = 0$), where $\mathrm{Im}[F] = 0$. The behavior (42) of $F(\gamma)$, in the vicinity of the points D and B, leads to the two following limiting behaviors of $\Phi(\zeta)$:

$$\Phi(\zeta) \approx \beta_D + \alpha_D(\zeta - \xi_D)^{(1/2)(1-\lambda)} \quad \text{as } \zeta \to \xi_D, \tag{59}$$

$$\Phi(\zeta) \approx \beta_B - \alpha_B(-\zeta - \xi_B)^{(1/2)(1+\lambda)} \quad \text{as } \zeta \to -\xi_B, \tag{60}$$

where β_B and β_D are real unknown constants, and α_B and α_D are real constants given by

$$\alpha_D = \frac{2^{\lambda/2}(\xi_D + \xi_B)^{(1+\lambda)/2}}{(1-\xi_D^2)^{(1-\lambda)/2}(1 + \xi_B\xi_D + \sqrt{(1-\xi_B^2)(1-\xi_D^2)})^{(1+\lambda)/2}}, \tag{61}$$

$$\alpha_B = \frac{(\xi_B + \xi_D)^{(1-\lambda)/2}}{2^{\lambda/2}(1-\xi_B^2)^{(1+\lambda)/2}(1 + \xi_B\xi_D + \sqrt{(1-\xi_B^2)(1-\xi_D^2)})^{(1-\lambda)/2}}. \tag{62}$$

On the other hand, using Eq. (54), the behavior (44) of $F(\gamma)$ when $\gamma \to \gamma_C$ imposes the following behavior of $\Phi(\zeta)$ in the ζ-plane:

$$\Phi(\zeta) \simeq \frac{\mathrm{i}\alpha}{\zeta^2}(1+\beta\zeta) + O(\zeta^0) \quad \text{as } \zeta \to 0, \tag{63}$$

where α and β are real constants given by

$$\alpha = \frac{2a}{\gamma_2} = \frac{2\sqrt{\cosh b}}{\gamma_2 \sinh b}\frac{K'}{K_o}, \tag{64}$$

$$\beta = -\frac{\gamma_3}{3\gamma_2} = -\frac{2}{3}\left[\frac{1}{\xi_D} - \frac{1}{\xi_B}\right]. \tag{65}$$

In the region $-\xi_B < \xi < \xi_D$, the function Φ satisfies an integral equation given by the transformation of Eq. (50) in the ζ-plane.

4.3. A practical representation of the solution $\Phi(\zeta)$

It is possible to write a representation of $\Phi(\zeta)$, which satisfies the boundary conditions (57) and (58), and has the appropriate limiting behaviors of Eqs. (59), (60) and (63). Let us write a priori $\Phi(\zeta)$ as (Muskhelishvili, 1953)

$$\Phi(\zeta) = \alpha[\Phi_1(\zeta) + \Phi_2(\zeta)], \tag{66}$$

with α the constant of Eq. (64) that is proportional to the stress intensity factor K', and where $\Phi_1(\zeta)$ and $\Phi_2(\zeta)$ are two holomorphic functions for $\eta > 0$ given by

$$\Phi_1(\zeta) = \frac{a_0}{\zeta^2} + \frac{a_1}{\zeta} + \left[\frac{b_0}{\zeta^2} + \frac{b_1}{\zeta}\right]\Omega(\zeta), \tag{67}$$

$$\Phi_2(\zeta) = \int_{-\xi_B}^{\xi_D} \frac{\Omega_R(t)\psi(t)}{t-\zeta}\,\mathrm{d}t, \tag{68}$$

where

$$\Omega(\zeta) \equiv (\zeta - \xi_D)^{(1/2)(1-\lambda)}(\zeta + \xi_B)^{(1/2)(1+\lambda)}, \tag{69}$$

$$\Omega_R(t) \equiv (\xi_D - t)^{(1/2)(1-\lambda)}(\xi_B + t)^{(1/2)(1+\lambda)}. \tag{70}$$

Here, a_j and b_j are real constants, and $\psi(t)$ is a real continuous function in the interval $[-\xi_B, \xi_D]$. Written in the forms (67) and (68), the functions $\Phi_1(\zeta)$ and $\Phi_2(\zeta)$, and consequently $\Phi(\zeta)$, satisfy automatically condition (57). Moreover, when $|\zeta| \to \infty$, condition (58) is satisfied since all the constants a_1, a_2, b_1, b_2 are real, as well as $\psi(t)$. The real constants a_j and b_j are determined by condition (63) satisfied by $\Phi(\zeta)$, and consequently by $\Phi_1(\zeta)$, in the vicinity of $\zeta = 0$. After simple algebraic manipulations one finds that

$$a_0 = -\tan[\lambda\pi/2], \tag{71}$$

$$b_0 = \frac{\sec[\lambda\pi/2]}{\xi_B^{(1+\lambda)/2}\,\xi_D^{(1-\lambda)/2}}, \tag{72}$$

$$a_1 = \beta a_0, \tag{73}$$

$$b_1 = \left[\beta + \frac{1-\lambda}{2\xi_D} - \frac{1+\lambda}{2\xi_B}\right] b_0. \tag{74}$$

The power law behavior of $\Phi(\zeta)$ for ζ close to $-\xi_B$ and ξ_D, as given by Eqs. (59) and (60), is readily satisfied by $\Phi_1(\zeta)$. On the other hand, the function $\Phi_2(\zeta)$ is the most general representation of an analytic function in the upper half-plane that satisfies the required behavior at $\zeta \simeq -\xi_B$ and at $\zeta \simeq \xi_D$, and whose imaginary part is zero on the segments of the real axis $\xi > \xi_D$ and $\xi < -\xi_B$. Indeed, for $-\xi_B < \xi < \xi_D$, one has (Muskhelishvili, 1953)

$$\mathrm{Im}[\Phi_2(\xi + \mathrm{i}\varepsilon)] = \frac{1}{2\mathrm{i}}[\Phi_2(\xi + \mathrm{i}\varepsilon) - \overline{\Phi_2}(\xi - \mathrm{i}\varepsilon)] = \pi\Omega_R(\xi)\psi(\xi), \tag{75}$$

a simple relation that guarantees the right behavior of $\Phi(\zeta)$ in the vicinity of the points B and D, and which also fixes, through Eqs. (59) and (60), the values of $\psi(-\xi_B)$ and $\psi(\xi_D)$.

Notice that the behavior of $\Phi(\zeta)$ for $\zeta \simeq 0$, as given by Eq. (63), is related to the behavior of $\psi(\xi)$ for $\xi \simeq 0$. Furthermore, let us recall that expansion (63) of $\Phi(\zeta)$ is prescribed by expansion (31) of the stress field S in the vicinity of the crack tip, where logarithmic singularities of the form $\log(b-s)$ and terms of the form $(b-s)^\mu$, with $-1/2 < \mu < 1/2$, are forbidden. Since the singular parts of $\Phi(\zeta)$ are already embedded in the function $\Phi_1(\zeta)$, the function $\Phi_2(\zeta)$ must not exhibit poles or singular behavior at $\zeta \simeq 0$. This result imposes that the function $\psi(\xi)$ must be of class C^1 for all $-\xi_B < \xi < \xi_D$ (i.e. continuous and with first derivative also continuous). This condition will be used in our numerical study in order to identify the proper stress intensity factor of the kinking problem.

Therefore, the problem of determining the solution $\Phi(\zeta)$ is now reduced to the determination of the real function $\psi(t)$ and of the real constant α. They are fixed by the integral equation (50) satisfied by Φ (or $\psi(t)$) in the region $-\xi_B < \xi < \xi_D$, combined with the complementary condition of the function $\psi(t)$ being of class C^1. Once the constant α is determined by this procedure, the stress intensity factor just after kinking is determined through the relation

$$\frac{K'(\lambda, v')}{K_o} \equiv H_{33}(\lambda, v'/c) = \frac{\sinh b}{\sqrt{\cosh b}}\, a = \frac{\sinh b}{2\sqrt{\cosh b}}\,\gamma_2\,\alpha. \tag{76}$$

A complete analytical solution cannot be derived in the general case. For the straight crack case ($\lambda=0$), one can easily verify that the exact solution as found by Eshelby and Kostrov (Kostrov, 1966; Eshelby, 1969), is given in our approach by $\psi(t) = 0$ and a stress intensity factor $K' = K_0\sqrt{1-v/c}$. For the general case, this problem will be solved numerically in the next section.

5. The stress intensity factor of the kinked crack

In our representation, the numerical problem consists in finding the function $\psi(t)$ and the real constant α using Eq. (50) and the condition of $\psi(t)$ being of class C^1. Except for α, the number of unknowns is equal to the number of available equations. Due to the presence of a singular behavior in the vicinity of the crack tip, and for numerical purpose, we modify in the following Eq. (50) into a more suitable integral equation.

Using Eq. (43), one can subtract the square root singular behavior in the integral equation (50), when $s \simeq b$. This leads to

$$\sqrt{\cosh s - \cosh b}[\mathrm{Im}[F(s + \mathrm{i}(\lambda\pi \pm \varepsilon))] - G(s)] = \cos\frac{\lambda\pi}{2} - \sqrt{2}a\cosh(b/2)$$
$$- \int_0^b \frac{\sqrt{\cosh b - \cosh s'}}{\cosh s - \cosh s'}\sinh s'[\mathrm{Im}[F(s' + \mathrm{i}\lambda\pi)] - G(s')]\,\frac{\mathrm{d}s'}{\pi}, \tag{77}$$

where

$$G(s) = \frac{2a\sinh(s/2)\cosh(b/2)}{\cosh s - \cosh b}. \tag{78}$$

The integral appearing in the integral equation (77) can be written in a different form in order to avoid a numerical singularity when $s \simeq s' \simeq b$. The integral is first written using a complex variable representation as

$$I(s) \equiv \int_0^b \frac{\sqrt{\cosh b - \cosh s'}}{\cosh s - \cosh s'}\sinh s'[\mathrm{Im}\,[F(s' + \mathrm{i}\lambda\pi)] - G(s')]\,\frac{\mathrm{d}s'}{\pi}$$
$$= \mathrm{Im}\int_\Gamma \frac{\sqrt{\cosh b - \cosh(\gamma - \mathrm{i}\lambda\pi)}}{\cosh s - \cosh(\gamma - \mathrm{i}\lambda\pi)}\sinh(\gamma - \mathrm{i}\lambda\pi)[F(\gamma) - \mathrm{i}G(\gamma - \mathrm{i}\lambda\pi)]\frac{\mathrm{d}\gamma}{\pi}, \tag{79}$$

where Γ is a curve in γ-space, with $\gamma = s' + \mathrm{i}\lambda\pi$ and $0 \leqslant s' \leqslant b$. This integration over Γ is now written in ζ-space, where the curve Γ starts on the ξ axis at the point F, enters into the upper half-plane and finishes at the point C that corresponds to the crack tip. Useful in this transformation of variables is the expression for $\gamma'(\zeta) = \mathrm{d}\gamma/\mathrm{d}\zeta$:

$$\gamma'(\zeta) = \frac{\mathrm{d}\gamma}{\mathrm{d}\zeta} = \frac{\gamma_2\zeta}{(1 + \zeta/\xi_B)(1 - \zeta/\xi_D)\sqrt{1 - \zeta^2}}. \tag{80}$$

Since the integrand of (79) is an analytic function for $\mathrm{Im}[\zeta] > 0$, the contour of integration Γ in ζ-space can be deformed. Closing the integral with a segment on the ξ axis from F to infinity and then with quarter of a circle at infinity and finishing with the

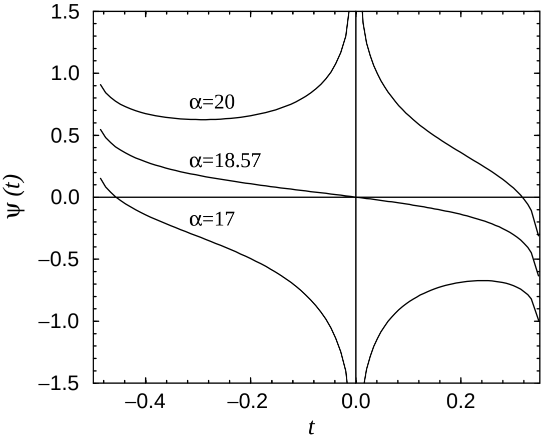

Fig. 4. Plot of the function $\psi(t)$ for $\lambda = 0.2$, $v'/c = 0.1$, and for different values of α.

vertical axis $\xi = 0$, one finds that the first two segments do not contribute, and the integral becomes

$$I(s) = -\mathrm{Im}\int_0^{\infty} \frac{\mathrm{i}d\eta}{\pi}\,\frac{\sqrt{\cosh b - \cosh(\gamma(\mathrm{i}\eta) - \mathrm{i}\lambda\pi)}}{\cosh s - \cosh(\gamma(\mathrm{i}\eta) - \mathrm{i}\lambda\pi)}\sinh(\gamma(\mathrm{i}\eta) - \mathrm{i}\lambda\pi)\gamma'(\mathrm{i}\eta)$$
$$\times[F(\gamma(\mathrm{i}\eta)) - \mathrm{i}G(\gamma(\mathrm{i}\eta) - \mathrm{i}\lambda\pi)]. \qquad (81)$$

Using this new representation of the integral, the numerical resolution of Eq. (50) can be done without difficulty. For each value of α, one finds a function $\psi(t)$ that satisfies the integral equation (77), and one varies α until the condition of no singular behavior of $\psi(t)$ (or $\psi(t)$ of class C^1) at $t = 0$ is satisfied. The corresponding value of α being the one we are looking for. In Fig. 4, we show examples of functions $\psi(t)$ for fixed values of λ and v' and for different values of α. It is seen that $\psi(t)$ presents a singularity at $t = 0$ that is incompatible with the physical expansion (17) of the stress field in the vicinity of the crack tip. This singularity is absent for a unique value of α, the desired one, where the function $\psi(t)$ satisfies the condition of being of class C^1. In Fig. 5, we plot the stress intensity factor K' as function of the kinking angle and for different velocities.

6. Discussion

In this paper, we presented a general method for determining the elasto-dynamic stress fields associated with the propagation of anti-plane kinked or branched cracks. As a first illustration, we considered a semi-infinite anti-plane straight crack, initially propagating at a given time-dependent velocity, that changes instantaneously both its direction and its speed of propagation. This work can be considered as a continuation and a generalization of the works on equilibrium of star shaped cracks, cases that

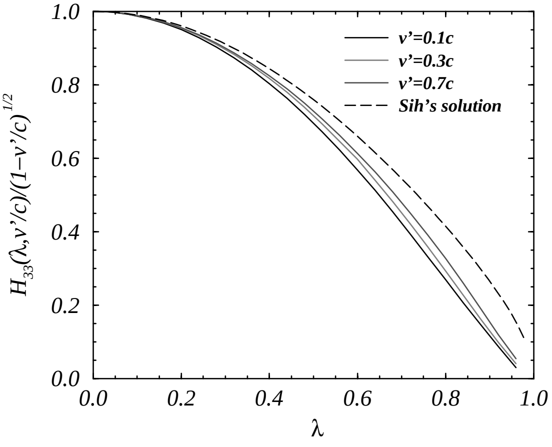

Fig. 5. Plot of the stress intensity factor function H_{33} as a function of the kinking angle and for different values of the crack tip velocity. Also shown in this figure, Sih's solution associated with the elasto-static kinking problem (Sih, 1965).

have been extensively studied (Sih, 1965; Amestoy and Leblond, 1992). It is also a generalization of the solutions found by Eshelby and Kostrov for the mode III straight dynamic crack (Eshelby, 1969; Kostrov, 1966, 1975; Freund, 1990). It also extends the class of self-similar solutions that were found for crack problems (Dempsey et al., 1982; Broberg, 1999; Willis, 1973).

Our approach allowed the exact calculation of the dynamic stress intensity factor for the dynamical kinked crack problem. The most important result of this study is displayed in Fig. 5. It is shown that our solution for vanishingly small velocity is different from the elasto-static solution, as given by Sih (1965), where the static stress intensity factor just after kinking, K_s', is related to the one just before kinking, K_0, by

$$K_s' = \left(\frac{1-\lambda}{1+\lambda}\right)^{\lambda/2} K_0. \tag{82}$$

This discrepancy was to be expected, since in this case the length of the kink is not time dependent and the propagating wave character of the solution is lost. Indeed, in Sih's solution, any small kink will modify the stress field all throughout the material, while in our representation of the kinking mechanism, the stress field is modified only within a cylindrical region limited by the cylindrical wave ct. Outside this region, the stress field remains unchanged with respect to the kinking process. Therefore, the propagation of bifurcated cracks should be seen as an intrinsically time dependent process, even if it occurs at vanishingly small speeds.

Although the equivalent in-plane dynamical kinked crack solutions remain to be found, the observed discrepancy between the elasto-static solution and the elasto-dynamic one with vanishingly small velocity, is expected to persist in that case also. Therefore, criteria of the path selection, such as the principle of local symmetry or the maximum energy release rate criterion, that have been developed for quasi-static crack propagation, using elasto-static solutions (Amestoy and Leblond, 1992; Leblond, 1989) be reviewed at least for quantitative facts.

In order to study the dynamic branching instability, the next step of this work will be the determination of the stress fields associated with the anti-plane symmetrical branching problem.

Acknowledgements

M.A.-B. wishes to thank M. Ben Amar and J.R. Rice for enlightening discussions. This work was financed by an international collaboration CNRS-CONICYT. Laboratoire de Physique Statistique de l'Ecole Normale Supérieure is associé au CNRS (UMR 8550), et aux Universités Paris VI et Paris VII.

References

Amestoy, M., Leblond, J.B., 1992. Crack paths in plane situations—II. Detailed form of the expansion of the stress intensity factors. Int. J. Solids Struct. 29 (4), 465–501.

Broberg, K.B., 1999. Cracks and Fracture. Academic Press, London.

Burgers, P., 1982. Dynamic propagation of a kinked or bifurcated crack in antiplane strain. J. Appl. Mech. 49, 371–376.

Burgers, P., 1983. Dynamic kinking of a crack in plane strain. Int. J. Solids Struct. 19, 735–752.

Dempsey, J.P., Kuo, M.K., Achenbach, J.D., 1982. Mode III kinking under stress wave loading. Wave Motion 4, 181–190.

Eshelby, J.D., 1969. The elastic field of a crack extending nonuniformly under general anti-plane loading. J. Mech. Phys. Solids 17, 177–199.

Freund, L.B., 1990. Dynamic Fracture Mechanics. Cambridge University Press, New York.

Gradshteyn, I.S., Ryzhik, I.M., 1994. In: Jeffrey, A. (Ed.), Table of Integrals, Series, and Products, 5th Edition. Academic Press, New York.

Kostrov, B.V., 1966. Unsteady propagation of longitudinal shear cracks. Appl. Math. Mech. 30, 1241–1248.

Kostrov, B.V., 1975. On the crack propagation with variable velocity. Int. J. Fracture 11, 47–56.

Lawn, B., 1993. Fracture of Brittle Solids. Cambridge University Press, New York.

Leblond, J.B., 1989. Crack paths in plane situations—I. General form of the expansion of the stress intensity factors. Int. J. Solids Struct. 25, 1311–1325.

Muskhelishvili, N.I., 1953. Some Basic Problems of the Mathematical Theory of Elasticity. Noordhoff, Groningen.

Ravi-Chandar, K., Knauss, W.G., 1984. An experimental investigation into dynamic fracture—III. On steady-state crack propagation and crack branching. Int. J. Fracture 26, 141–154.

Sharon, E., Fineberg, J., 1996. Microbranching instability and the dynamic fracture of brittle materials. Phys. Rev. B 54, 7128–7139.

Sharon, E., Fineberg, J., 1999. Confirming the continuum theory of dynamic brittle fracture for fast cracks. Nature 397, 333–335.

Sih, G.C., 1965. Stress distribution near internal crack tips for longitudinal shear problems. J. Appl. Mech. 32, 51–58.

Williams, M.L., 1952. Stress singularities resulting from various boundary conditions in angular corners of plates in extension. J. Appl. Mech. 19, 526–528.

Willis, J.R., 1973. Self-similar problems in elastodynamics. Philos. Trans. R. Soc. (London) 274, 435–491.